RECEIVER OPTIMIZATION FOR L-DACS1

U. Epple, S. Brandes, S. Gligorevic, M. Schnell, German Aerospace Center (DLR), Germany

Abstract

L-DACS1 is the broadband candidate technology for the future L-band Digital Aeronautical Communications System (L-DACS). The flexible design of L-DACS1 allows the deployment as an inlay system in the spectral gaps between two adjacent channels used by the Distance Measuring Equipment (DME) as well as the non-inlay deployment in unused parts of the L-band. In this paper, the synchronization procedure in L-DACS1, when deploying it as inlay system is presented. It will be investigated how the synchronization suffers from interference in the L-band. In addition, interference mitigation techniques are briefly described and their influence onto the synchronization is examined. Finally, the performance of an appropriate combination of interference mitigation and robust synchronization is presented, showing that even under severe interference conditions, a reliable synchronization can be accomplished, hence confirming the feasibility of the inlay concept.

Introduction

The future communication study (FCS) jointly carried out by FAA and Eurocontrol has identified two candidates for the future aeronautical communication system in the L-band. One candidate is a broadband multi-carrier system employing orthogonal frequency-division multiplexing (OFDM) referred to as L-DACS1. The other one is a narrowband single-carrier system referred to as L-DACS2. The FCS has recommended follow-on activities in order to specify the proposed L-DACS options and validate their performance with the goal to finally decide for one candidate by 2010 [1]. These activities should be conducted within future research programs, i.e. Single European Sky ATM Research (SESAR) in Europe and NextGen in the USA.

For L-DACS1, which is addressed in this paper, a combination of P34 (TIA 902 standard) [1] and the Broadband Aeronautical Multi-carrier Communications (B-AMC) system [3]-[5] has been anticipated. Initiated by Eurocontrol, the specification of L-DACS1 has been started in 2008 and a first version of the specification is available since beginning of 2009 [6].

L-DACS1 is a multi-application cellular broadband air-ground system capable of simultaneously providing various kinds of Air Traffic Services (ATS) and Aeronautical Operational Control (AOC) communications services. It is designed to fulfill the requirements of the future aeronautical communication system as defined in [7].

L-DACS1 is intended to be operated in the aeronautical part of the L-band (960-1164 MHz). The frequency band is mainly utilized by aeronautical navigation aids such as the distance measuring equipment (DME) or the military Tactical Air Navigation (TACAN) system. In addition, in some countries parts of this band are used by the military Multifunctional Information Distribution System (MIDS) or the Joint Tactical Information Distribution System (JTIDS). Several fixed channels are allocated for the Universal Access Transceiver (UAT) at 978 MHz and for Secondary Surveillance Radar (SSR)/Airborne Collision Avoidance System (ACAS) at 1030 and 1090 MHz. On the last World Radio Conference in 2007, this frequency band has also been assigned to aeronautical communication systems which may coexist with other L-band systems on a non-interfering basis.

Taking into account these constrains, L-DACS1 is designed to provide three different deployment options. One conventional approach is deploying L-DACS1 in a free sub-band of the aeronautical L-band which is exclusively assigned to the aeronautical communication system. However, due to the many existing L-band systems it might be difficult to allocate new spectrum. A second option is the so-called inlay approach where L-DACS1 is operated in the spectral gaps between two adjacent DME or TACAN channels. This approach is especially attractive since it does not require the assignment of any new spectrum and the existing spectrum allocation of all other L-band systems can be retained. The third option is a combination of the first two concepts. Since in L-DACS1 forward and reverse link (FL/RL) are separated by frequency-division duplex (FDD), the FL

might be deployed in free spectrum and the inlay approach might be applied for the RL or vice versa.

Although being very promising, the inlay concept poses special challenges to the design of the physical layer. The transmitter (Tx) may not cause harmful interference at other L-band systems. Countermeasures for reducing out-of-band radiation have been proposed in [3]. The L-DACS1 receiver (Rx) has to be robust towards interference from other L-band systems. Due to the high interference power and small frequency offset between L-DACS1 and other L-band systems, interference strongly impairs the L-DACS1 Rx signal. Techniques for mitigating the impact of interference and a robust algorithm for channel estimation have been addressed in [8] and [9], respectively. In this paper, the synchronization in time and frequency between the L-DACS1 Tx and Rx is investigated and a synchronization algorithm which is robust towards interference is proposed.

The remainder of this paper is organized as follows. At first, the elements of the physical layer design relevant for synchronization are briefly recapitulated. After analyzing interference conditions related to the inlay deployment concept, an appropriate synchronization algorithm in combination with techniques for interference mitigation is presented. The performance of the proposed algorithm is demonstrated by means of simulations in a realistic interference scenario. The paper ends with conclusions and an outlook on future work.

System Design

The L-DACS1 physical layer is based on OFDM modulation and designed for operation in the aeronautical L-band. In order to maximize the capacity per channel and optimally use the available spectrum, L-DACS1 is defined as a FDD system supporting simultaneous transmission in FL and RL channels, each with an effective bandwidth of 498.05 kHz.

L-DACS1 FL is a continuous OFDM transmission. Broadcast and addressed user data are transmitted on a (logical) data channel; dedicated control and signaling information is transmitted on (logical) control channels. The capacity/size of the data and the control channel changes according to system loading and service requirements. Message based adaptive transmission data profiling with adjustable modulation and coding parameters is supported for the data channels in FL and RL.

L-DACS1 RL is based on Orthogonal Frequency-Division Multiple-Access / Time-Division Multiple-Access (OFDMA-TDMA) bursts assigned to different users on demand. In particular, the RL data and the control segments are divided into tiles, hence allowing the medium-access control (MAC) sub-layer of the data link layer the optimization of resource assignments as well as the control of bandwidth and duty cycle according to the interference conditions.

OFDM Parameters

The channel bandwidth of 498.05 kHz is used by an OFDM system with 50 sub-carriers, resulting in a sub-carrier spacing of 9.765625 kHz. This sub-carrier spacing was chosen as a trade-off between a high spectral efficiency and an acceptable inter-carrier-interference (ICI) caused by Doppler shifts of up to 1.25 kHz, typically occurring in the aeronautical environment.

For OFDM modulation, a 64-point FFT is used. The total FFT bandwidth comprising all sub-carriers is 625.0 kHz. Besides the 50 sub-carriers used for transmission, the 64 FFT comprise one direct current (DC) sub-carrier as well as seven empty sub-carrier at the left edge of the spectrum and six at the right edge, serving as guard bands.

According to the sub-carrier spacing, one OFDM symbol has a duration of 102.4 μs. Each OFDM symbol is extended by a cyclic prefix of 17.6 μs, comprising a guard interval of 4.8 μs as well as 12.8 μs for Tx windowing. The guard interval provides resistance to inter-symbol interference caused by multipath effects. Tx windowing leads to a reduction of out-of-band radiation. This results in a total OFDM symbol duration of 120 μs. The main L-DACS1 OFDM parameters are listed in Table 1.

With respect to synchronization the sub-carrier spacing is a measure for the maximum frequency error that can be compensated by the synchronization procedure at Rx. Errors of the time synchronization will lead to no degradation, if they are less than the guard interval.

Table 1: Main L-DACS1 OFDM Parameters

Parameter	Value

Parameter	Value
Effective bandwidth (FL or RL)	498.05 kHz
Sub-carrier spacing	9.765625 kHz
Used sub-carriers	50
FFT length	64
OFDM symbol duration	102.4 µs
Cyclic prefix - guard time - windowing time	17.6 µs 4.8 µs 12.8 µs
Total OFDM symbol duration	120 µs

Framing Structure

OFDM symbols are organized into OFDM frames. Depending on their functionality, different frame types are distinguished. The frames are arranged into Multi-Frames (MF) and Super-Frames (SF). The structure of a SF is depicted in Figure 1. Based on this structure, the different frame types shall be described mainly focusing on the synchronization procedure and the maintenance of a synchronous transmission of the ground station (GS) and the airborne stations (AS). More detailed information on the different frame types can be found e.g. in [5] and [9].

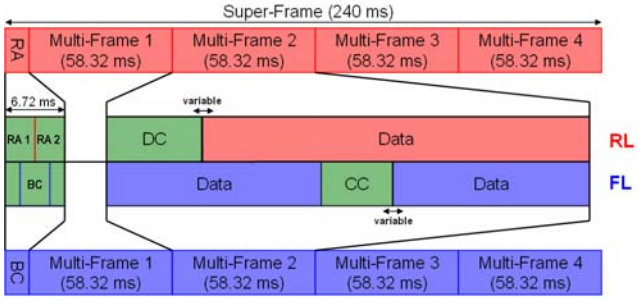

Figure 1: Super-Frame Structure

One SF contains of one Broadcast (BC) Frame in the FL and of one Random Access (RA) Frame in the RL, respectively, and of four MF in both, FL and RL. FL and RL have to be synchronous at the beginning of a SF. As, the GS provides the global timing reference the ASs has to synchronize themselves to the GS. The synchronization procedure is presented in the following, based on the synchronization opportunities which are provided by the different frame types.

FL BC Frame

The BC Frame is divided into three sub-frames BC1, BC2 and BC3, which are depicted in Figure 2. Besides the DC sub-carrier and the guard bands, 50 sub-carriers for data-transmission are available. For applying data-aided channel estimation at Rx, pilot symbols are inserted into the time-frequency-plane.

Each of the three sub-frames starts with two OFDM symbols, comprising synchronization sequences. Before executing a net-entry, an AS has to obtain an initial time synchronization, based on these synchronization symbols. Due to the irregular intervals between the synchronization symbols in the sub-frames which are 1.8 ms between BC1 and BC2 and 3.12 ms between BC2 and BC3, respectively, the synchronization is unambiguous.

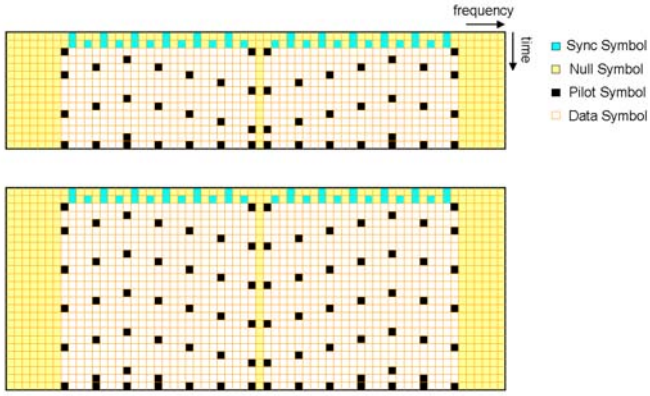

Figure 2: Structure of BC1 and BC3 Sub-Frames (above) and BC2 Sub-Frame (below)

RL RA Frame

Based on this initial time synchronization, the AS can send a net-entry request at the right moment in one of the RA sub-frames given in Figure 3. As the distance between the GS and the AS is still unknown, each sub-frame is surrounded by guard times of 1.26 ms to counterbalance the propagation delay of the maximal AS-GS distance of 200 nm.

Figure 3: RA Access Opportunities

Each RA sub-frame (Figure 4) starts with a preamble OFDM symbol, used for a fast automatic gain control (AGC) at Rx, which is needed due to the preceding guard time, where no data is transmitted. This preamble is followed by two synchronization symbols and four OFDM data symbols, used for control information concerning the net-entry.

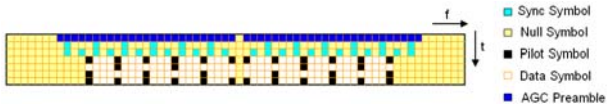

Figure 4: RL RA Sub-Frame

FL Data/CC Frame

In the FL, each SF frame consists, besides the BC frame of four MFs. One MF itself comprises nine Data/CC frames, which are used to transmit control information and user data to the ASs. Each Data/CC frame starts with two synchronization symbols as depicted in Figure 5. These OFDM synchronization symbols are used in the AS to update the initial synchronization got by the BC frame.

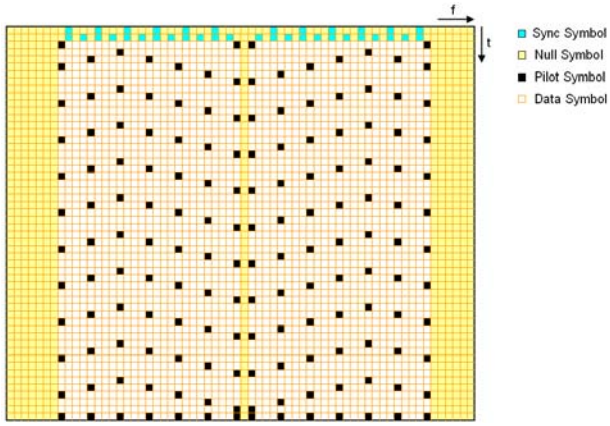

Figure 5: Structure of an FL Data/CC Frame

RL DC Segment

In the RL, no simple synchronization like in the FL is possible, as several ASs with different frequency offsets and distances, thus different transmission delays, share the same transmission bandwidth. To obtain a synchronized reception of the different ASs at the GS Rx, a pre-compensation of the expected time and frequency offsets has to be applied in the AS Tx in advance. These offsets are measured in the GS, exploiting the two synchronization symbolsin the RA sub-frame when an AS accomplishes a net-entry. The time and frequency offset are tracked in the AS Rx, using the synchronization symbols in the FL Data/CC Frames. However, since a tracking can lead to an accumulation of errors, an updating of the time and frequency offset has to be applied periodically. The synchronization symbols in the DC segments (see Figure 6) provide possibilities for several ASs to send a synchronization sequence, which will be exploited in the GS Rx. The updated values for timing and frequency offset will be communicated to the AS via the CC.

As the guard time of the RA frame may precede the DC segment, a preamble is inserted at the beginning, supporting the AGC in the GS Rx. The remainder of the DC segment is grouped into tiles. One tile is dedicated to one AS for requesting resources.

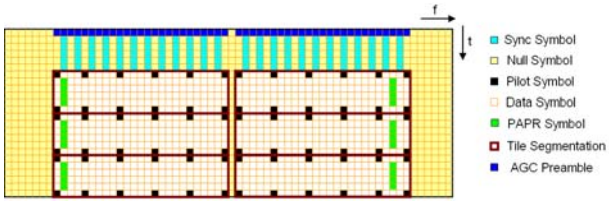

Figure 6: RL DC Segment

RL Data Segment

The RL Data Segment possesses the same tiles as the RL DC segment. However, it does not contain synchronization symbols at the beginning since the DC segments provide already enough possibilities for updating the synchronization of an AS.

Interference Scenario

When deployed as an inlay system DME/TACAN signals represent the most severe interference towards L-DACS1. Due to the mostly larger frequency separation between L-DACS1 and other interfering systems like JTIDS, UMTS or SSR, these systems will not be considered in the following.

Mathematically, a DME signal consists of pairs of Gaussian shaped pulses which are described by

$$p(t) = e^{-\alpha t^2/2} + e^{-\alpha (t-\Delta t)^2/2}.$$

The parameter Δt = 12 µs or 36 µs denotes the spacing of the pulses, the parameter α characterizes the width of one pulse. The used value $\alpha = 4.5 \cdot 10^{11} \cdot 1/s^2$ leads to a width of 3.5 µs at 50% of the maximum amplitude. Figure 7 clarifies the shape of one DME pulse pair and the given parameters.

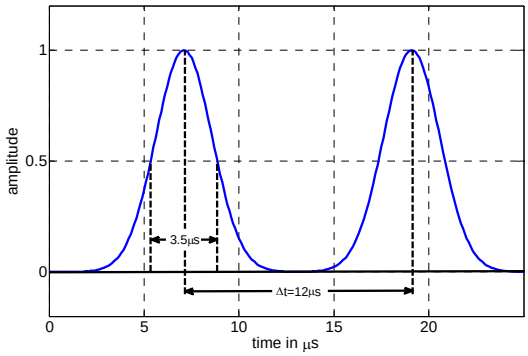

Figure 7: DME Pulse Pair in the Time Domain

A Gaussian shaped pulse leads also to Gaussian shaped spectrum. Since pulses are occurring pair-wise, the spectrum exhibits fades. The different DME channels operate on different frequencies with a spacing of multiples of 1 MHz. This leads to a DME spectrum in the aeronautical L-band as depicted in Figure 8 for a bandwidth of 4 MHz, i.e. 4 DME channels. L-DACS1 will operate as an inlay system between two adjacent DME channels. An example for this deployment concept is also given in Figure 8.

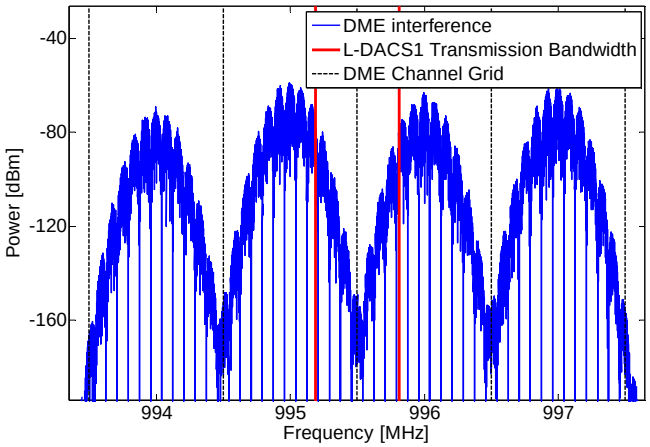

Figure 8: Spectrum of DME Pulses and L-DACS1 Transmission Bandwidth

For further investigation, a realistic DME interference model has to be used. As the L-DACS FL is intended to be operated in the sub-band 979-1025 MHz, except for the "own" airborne DME interrogator, which is neglected here, only DME GSs cause interference at the L-DACS1 AS Rx. The real DME channel allocation is modeled with the NAVSIM[1] tool [10] for the area around Paris as this is the area with the highest density of DME ground stations in Europe. The victim L-DACS1 Rx is positioned at an en-route (ENR) flight level at 45,000 feet altitude in the center of this area. The peak interference power originating from each DME/TACAN GS is determined via simple link budget calculations, taking into account free space loss and elevation angle dependent antenna gains that are derived from directive antennas of standard DME equipment. In this particular example, severe interference conditions are observed when L-DACS1 is operated at 995.5 MHz. In this scenario, only interferers in the channels at ± 0.5 MHz offset to the L-DACS1 center frequency are considered. Interference from DME stations in channels at larger offsets are supposed not to impair the L-DACS1 system significantly due to their larger separation in frequency and their spatial distance. The considered interference scenario is listed in Table 2.

[1] The Air Traffic / ATC & CNS simulation tool "NAVSIM" has been developed by "Mobile Communications R&D GmbH, Salzburg" in close co-operation with University of Salzburg.

Table 2: ENR Interference Scenario

Station	Frequency [MHz]	Interference power at victim RX input	Pulse rate (ppps)
TACAN	995	-67.9 dBm	3600
L-DACS1	995.5		
TACAN	996	-74.0 dBm	3600
TACAN	996	-90.3 dBm	3600

One TACAN GS may transmit up to 3600 pulse pairs per second (ppps). In the considered interference scenario, three TACAN GSs occur in both adjacent channels. As the pulses of the three stations are statistically independent, their pulse rates can be represented by one random process producing a total pulse rate as high as 10800 ppps. Modeling the starting times of the pulse pairs as a Poisson process, the probability that an OFDM symbol is hit by DME interference is given by the complementary probability of the event that no interference occurs within an OFDM symbol, i.e.

$$P_{hit} = 1 - e^{-\lambda (T_O + 3.5\,\mu s)}$$

with T_O denoting the duration of an OFDM symbol which is 96 µs for L-DACS1. Note, the cyclic prefix is neglected in this consideration, since it is discarded at the OFDM Rx anyway and pulses in the cyclic prefix do not impair the data bearing part of the OFDM symbol. However, the observed interval has to

be extended by the duration of one pulse to take into account pulses at the end of an OFDM symbol. The intensity λ of the Poisson process is determined by the number of pulses which is $2 \cdot 10800$ pulses per second in the regarded example. With the given parameters, the probability that an OFDM symbol is hit by DME interference (regardless of its power) is 88%. The probability that one OFDM symbol is hit by two pulses is as high as 25%. To overcome this deleterious impact onto L-DACS1, the receiver has to be designed accurately and with respect to the particular characteristics of the DME interference. In the following sections, the synchronization in the receiver and particular interference mitigation techniques are presented.

Receiver Design

Promising receiver techniques for reducing the deleterious influence of DME interference onto L-DACS1 have been proposed e.g. in [8] or [9]. However, these investigations are based on the assumption of perfect synchronization. In this section, the real synchronization procedure of time and frequency is presented. In addition, interference mitigation techniques will be shortly described, focusing on the interaction between them and synchronization.

Synchronization algorithm

For applying a synchronization in the receiver, special synchronization symbols, as depicted in Figure 9, are inserted in the FL frames (see Figure 2 and Figure 5).

Figure 9: Synchronization OFDM Symbols in the Frequency Domain

The occupation of every forth sub-carrier of the first synchronization symbol leads after the IFFT to a time domain waveform consisting of four identical parts. In the second synchronization symbol, every second sub-carrier is occupied leading to a time domain waveform with two identical parts. Both synchronization symbols in the time domain after adding the cyclic prefix and applying Tx windowing are depicted schematically in Figure 10.

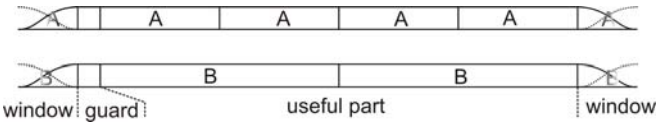

Figure 10: Synchronization OFDM Symbols in the Time Domain

The sub-carriers of the synchronization symbols are occupied with Chu-Sequences [11], leading to a low peak-to-average-power-ratio (PAPR) and good correlation properties.

This particular structure in the time domain is exploited in the receiver by applying an adequate correlation, which is described by

$$P(d) = \sum_{m=0}^{N_{corr}-1} \left(r^*(d+m) \cdot r\left(d+m+N_{diff}\right) \right).$$

with d being the time sample index of the discrete receive signal $r(d)$. As identical parts in both symbols possess a distance of half a symbol, the correlation difference N_{diff} is defined by $N_{diff} = N_{ov}\left(N_{fft}/2\right)$, with N_{ov} being the oversampling factor in the receiver (see [9]). The correlation should imply as many identical samples as possible, which leads to a correlation length of $N_{corr} = N_{ov}\left(N_{fft}/2 + N_g + N_w/2\right)$ due to the guard interval and windowing. This correlation slides along in time, i.e. the parameter d is increased, searching for peaks of the both synchronization symbols. To get a consistent measure for the significance of a peak, the correlation is normalized by

$$N(d) = \tfrac{1}{2} \sum_{m=0}^{N_{corr}-1} \left(\left|r(d+m)\right|^2 + \left|r\left(d+m+N_{diff}\right)\right|^2 \right),$$

leading to the timing metric

$$M(d) = \frac{\left|P(d)\right|^2}{N^2(d)}.$$

For a signal-to-noise ratio (SNR) of 10 dB in an additive white Gaussian noise (AWGN) channel, the timing metric is depicted in Figure 11 for both synchronization symbols. In the perfect case, the peaks of the metric occur at the position $d_0 = d_u - \left(N_g + N_w/4\right)N_{ov}$, with d_u denoting the beginning of the useful part of a synchronization symbol.

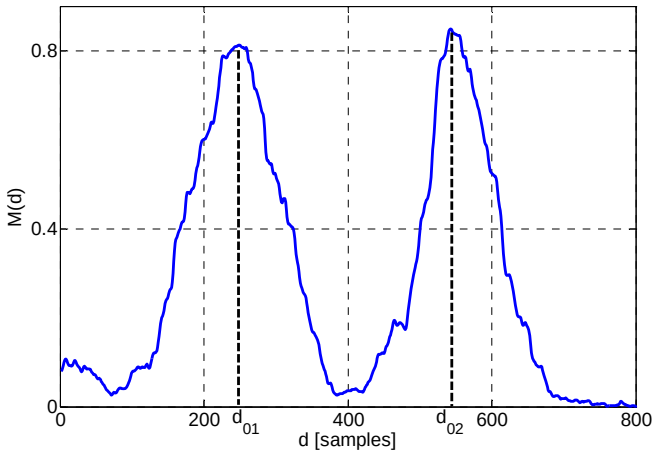

Figure 11: Timing Metric M(d)

The frequency synchronization is obtained by exploiting P(d). The Fourier correspondence says that a frequency offset leads to a rotation of the phase of the signal in the time domain:

$$S(f - f_0) \quad \bullet\!-\!\circ \quad s(t)\cdot\exp(j2\pi f_0 t).$$

This phase, again, corresponds to the angle of P(d), since the first and the second half of a synchronization symbol are created identically. Hence the frequency offset is calculated by

$$f_0 = \frac{1}{2\pi}\frac{N_{ov}N_{fft}}{N_{diff}} angle(P(d_0)).$$

In Figure 12, the angle of P(d) is depicted, as in Figure 11 at an SNR of 10dB in an AWGN channel. It can be well seen that the frequency offset is constant around d_0, thus a misalignment of the time synchronization does not necessarily lead to a corrupted frequency synchronization.

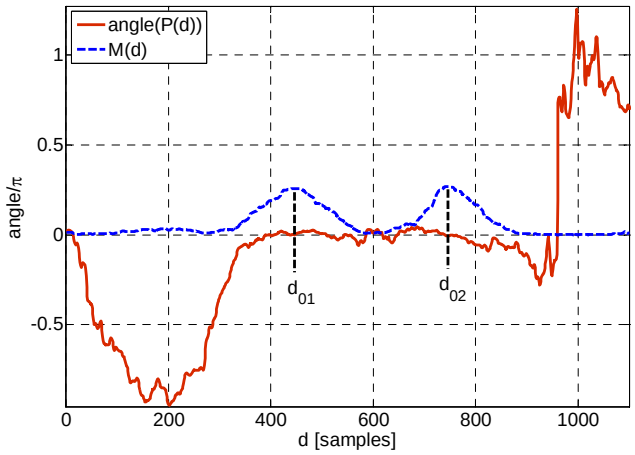

Figure 12: Angle of Correlation Function P(d)

These correlation metrics are similar to [12]. However, in opposite to [12], we obtain a unique peak and no uncertainty due to the plateau. In addition, the whole synchronization symbol is used for normalization. If only the second half, as in [12] was used, wrong peaks, originating from strong DME pulses in the first half of the synchronization symbol, could occur. Furthermore, our algorithm leads to peaks at both synchronization symbols, which is beneficial, as about 88% of all OFDM symbols will be hit by DME pulses (see section on interference).

For refining the synchronization results, an algorithm, proposed in [13] is applied. It exploits the cyclic prefix of an OFDM symbol by simply correlating it with its corresponding useful part. After this, the results of all OFDM symbols in one frame are averaged to get reliable values for the time and frequency offset of one frame.

Interference mitigation techniques

For mitigating the deleterious influence of DME interference onto L-DACS1, pulse blanking (PB) and pulse clipping (PC) as well as data erasure decoding have been investigated in [8]. In [9], pilot erasure setting has been investigated to improve the channel estimation. The advantage of the former technique is, that it can be applied in the time domain prior to synchronization and thus may have a beneficial influence onto the performance of the synchronization. Thus, in the remainder of the paper, only PB and PC will be investigated. Prior to blanking or clipping DME pulses, a reliable detection either based on a simple threshold decision or a correlation with a known DME pulse has to be carried out. In addition, a reasonable

threshold has to be defined as a trade-off between mitigation as much interference power as possible without loosing too much valuable data. These issues have been investigated in [14].

Figure 13 briefly shows the principle of pulse blanking and clipping. If the Rx signal exceeds a certain threshold and interference is detected the signal will be set to zero for that period in the case of pulse blanking. For pulse clipping, the magnitude of the signal will set to the threshold whereas the phase of the Rx signal is maintained.

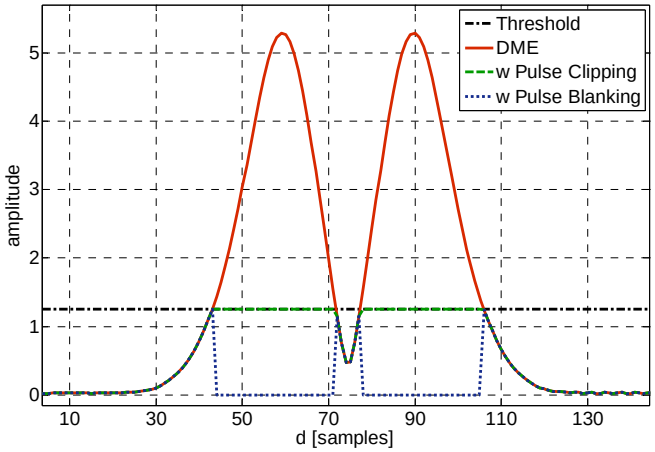

Figure 13: Principle of Pulse Blanking and Pulse Clipping

The beneficial influence of PB and PC onto the synchronization is shown in Figure 14. The peaks of the metric M(d) in the case of no interference almost vanishes if the synchronization symbols coincidence with DME interference. When PC is applied, small peaks become visible; when applying PB the metric M(d) shows again distinct peaks.

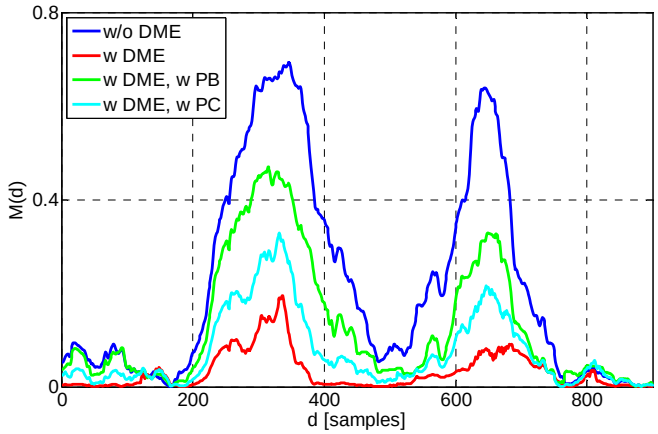

Figure 14: Influence of Pulse Blanking and Pulse Clipping onto Metric M(d)

To decide whether or not a peak is reliable, a threshold has to be defined. It has to be chosen carefully, as a too low threshold would lead to wrong peaks resulting from channel impairments, whereas with a too high threshold, many peaks of the metric would not be detected, although they might be reliable. In the next section, results simulated with different thresholds will be given and a appropriate threshold is determined.

Simulation Results

For all simulations with DME interference in the FL, the ENR scenario described in the interference section above is assumed.

For representing the aeronautical propagation channel environment, an ENR scenario has been applied. Besides a strong line-of-sight path, it comprises reflected paths with a delay of τ_1 = 0.3µs and τ_2 = 15µs. The maximal velocity of an AS in this scenario is 1360 km/h, corresponding to a maximal Doppler shift of 1250 Hz.

Figure 15 gives the average time until a synchronization in the AS Rx, based on BC frames is accomplished. For an accomplishment, M(d) has to exhibit peaks in distances of 1.8 ms and 3.12 ms, according to the duration of the BC sub-frames. As tolerance interval for the peaks, the duration of the cyclic prefix (17.6 µs) was chosen. As threshold for the reliability of the peaks, 0.4 has been taken.

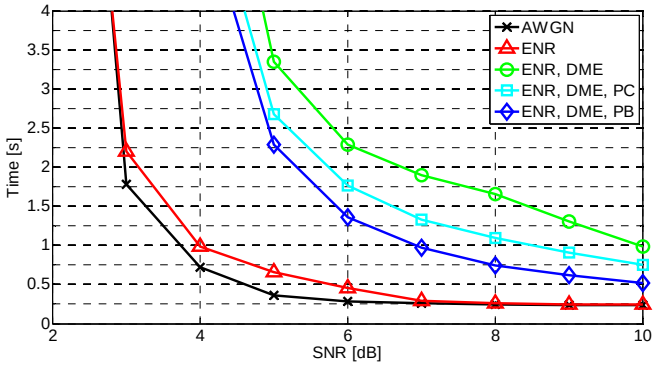

Figure 15: Average Time to Initial Synchronization base onto BC-Frames

If no interference occurs, for a SNR of 4dB or larger, the initial synchronization is accomplished in less then 1s for the AWGN as well as for the DME case without interference. The good performance of the ENR channel results from a strong line-of-sight (LOS) path. In the case of DME interference, the time till successful synchronization increases remarkably and at least a SNR of 6dB is needed to accomplish a synchronization within an acceptable time interval of 2.25s. By applying PC or PB, this time is decreased by 0.5s and 0.9s, respectively, resulting in an average time to initial synchronization of about 1.3s at SNR = 6dB when applying PB.

Based on these results, the synchronization in the FL data frames is investigated. In the following, only PB but no PC is applied, as it has a more beneficial influence on the synchronization in the case of interference. In Figure 16, the influence of the synchronization threshold onto the synchronization error rate in FL data frames is shown for the ENR channel and DME interference. For interference mitigation, PB is applied. The synchronization error rate is defined as the ratio between number of unsuccessful synchronizations at the beginning of FL Data/CC frames and the total number of synchronization opportunities. As expected, a lower threshold leads to a higher number of successful synchronizations. At SNR = 6dB, thresholds of 0.3 or 0.4 lead to acceptably low error rates below 0.3. However, a low threshold will also lead to wrong synchronizations due to peaks originating from interference.

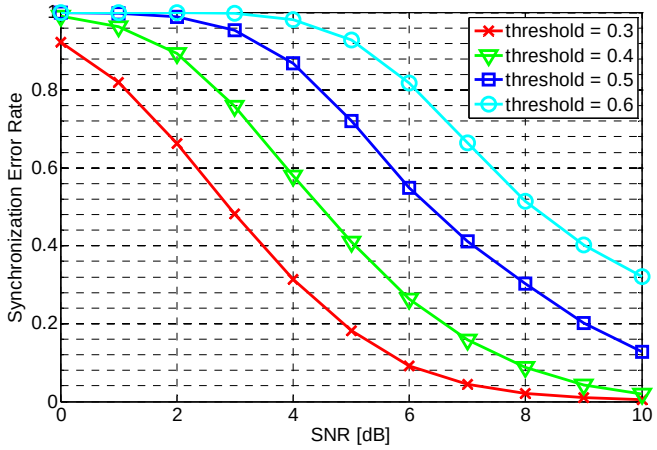

Figure 16: Influence of Synchronization Threshold onto the Synchronization Error Rate

The ratio of wrong peaks in Figure 17 shows the number of wrong peaks divided by the number of expected synchronization peaks. While a threshold of 0.2 leads to a wrong synchronization rate of almost 25%, with a threshold of 0.4 the rate is decreased to less than 2%. With a higher threshold, no wrong peaks occur. Keeping the synchronization error rate in mind, a threshold of 0.4 seems to be a good trade-off and will be used in the following.

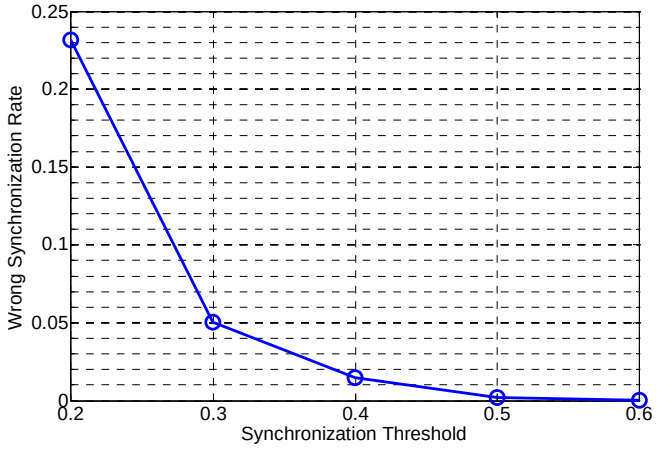

Figure 17: Influence of Synchronization Threshold onto the Wrong Synchronization Rate

Next, the influence of the number of synchronization symbols onto the synchronization error rate is regarded in Figure 18. It becomes clear that under such interference conditions the augmentation from one to two synchronization symbols is a suitable method to improve performance. When looking at an SNR of 6dB, the synchronization

error rate is reduced from 65% to 25% by increasing the number of synchronization symbols.

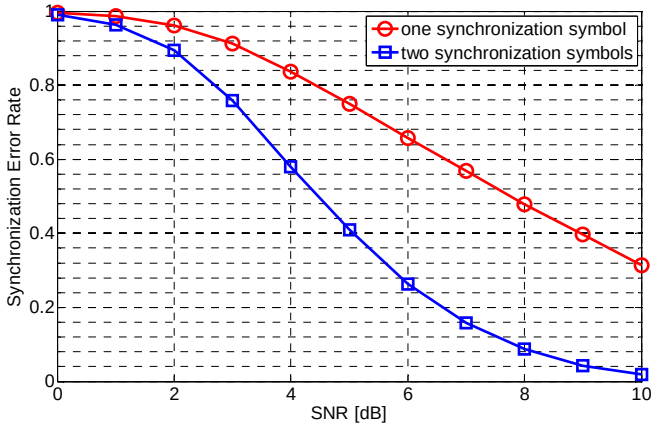

Figure 18: Influence of Number of Synchronization OFDM Symbols onto Synchronization Error Rate

Even if a synchronization in a FL Data/CC frame is successful, the performance of the exact time and frequency offset can vary, as the peak of M(d) may not be exactly at the correct position and the angle of P(d) may be corrupted by channel impairments. These effects are quantified in terms of the mean-square-error (MSE) between perfect and measured values. Figure 19 shows the MSE of the time synchronization in the FL Data/CC frames for the ENR channel, with and without interference and with and without PB. In addition, MSE curves are given when additionally applying the refining algorithm from [13]. For all MSE curves, only successful synchronizations are taken into account, as wrong peaks would dominate the MSE curves and the accuracy of the algorithm itself would not come visible.

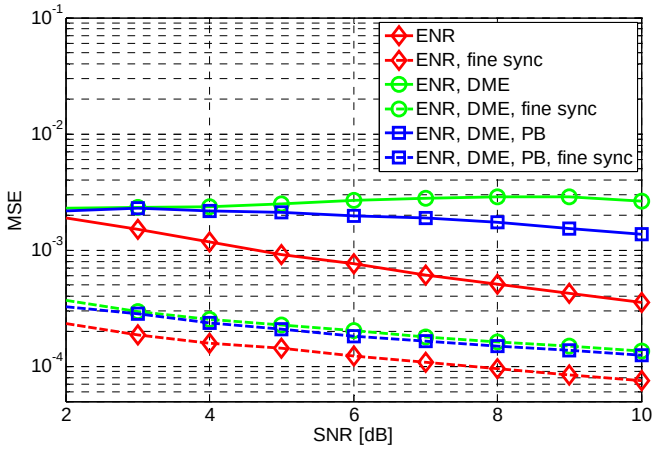

Figure 19: MSE of Time Synchronization

The results are in accordance with Figure 15. Interference leads to a significantly higher MSE compared to the interference-free case. When applying PB, the MSE is slightly reduced. The refinement algorithm leads in all cases to a large improvement of the MSE. If the error of time synchronization is within the cyclic prefix, it will not cause inter-symbol-interference (ISI), but only a rotation of the sub-carriers, which can be compensated by the channel estimation. Thus, with a MSE of $2 \cdot 10^{-4}$ for SNR = 6dB no degradation of the bit-error-rate (BER) is expected.

When looking at the MSE of the frequency synchronization, it should be as small as possible, since each misalignment of the carrier frequency will lead to inter-carrier-interference (ICI) when executing the FFT in the receiver. Figure 20 shows the MSE of the frequency synchronization. The results are similar to the MSE of time synchronization. Again, PB leads to a reduction of the MSE, however, it is marginal. Also, the refining algorithm leads to much lower MSE values.

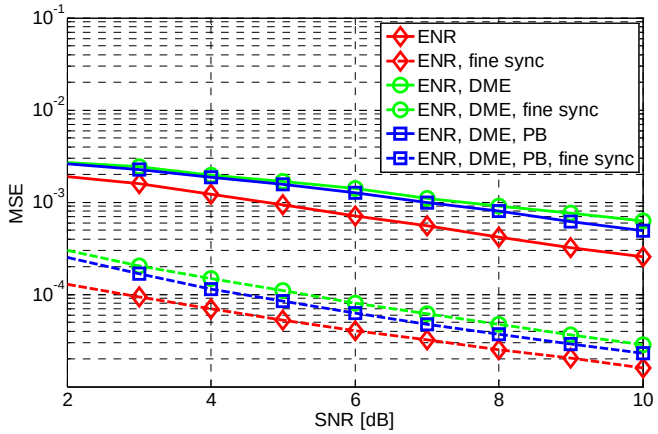

Figure 20: MSE of Frequency Synchronization

To appraise the influence of the remaining frequency error onto the overall performance of L-DACS1, BER curves are given in Figure 21. For the channel estimation, a pilot-based linear interpolation is applied. In addition, pilot boosting to a level of 2.5dB is used. Other improvements, such as pilot erasure setting (see [9]) have not been deployed, as they cannot be used in combination with PB.

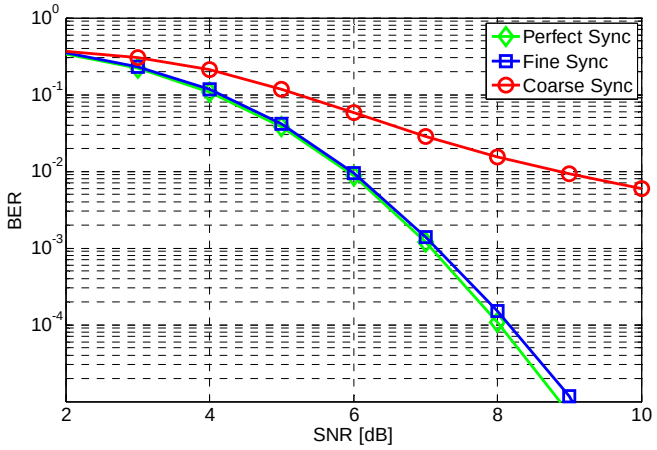

Figure 21: Influence of Synchronization onto BER

If no fine synchronization is applied, the synchronization errors lead to a remarkable degradation of the performance, resulting in an error floor at BER = $5 \cdot 10^{-3}$. However, when applying the refining algorithm, the perfect synchronization curve is almost reached, and only for high SNR values, a small degradation becomes visible.

Conclusions and Outlook

L-DACS1 is the broadband candidate for the future A/G communication system in the L-band. It is designed to meet the requirements of the future aeronautical communication system. The flexible design of L-DACS1 allows the deployment as an inlay system in the spectral gap between two adjacent DME channels as well as the deployment in unused spectrum.

In the first part of the paper, the framing structure of the system is described with respect to the synchronization procedure in the FL and RL. The different frame types are presented, focussing on the synchronization opportunities they provide.

The synchronization algorithm in the Rx is described in the second part. Appropriate correlation function as well as interference mitigation techniques and their beneficial influence on synchronization are presented. The synchronization algorithm can be further refined by exploiting the cyclic prefix. The performance of the synchronization is demonstrated under severe interference conditions, especially when applying interference mitigation. It could be shown, that a robust synchronization was developed, which will not degrade system performance.

For the future it is intended to develop more sophisticated interference mitigation techniques, which result in less bit errors, without loosing the robustness of the synchronization.

References

[1] AP17 Final Conclusions and Recommendations Report, EUROCONTROL/FAA/ NASA, v1.1, November 2007

[2] TIA standard family TIA-902, 2002/2003

[3] M. Schnell, S. Brandes, S. Gligorevic, C.-H. Rokitansky, M. Ehammer, Th. Gräupl, C. Rihacek, M. Sajatovic, "B-AMC – Broadband Aeronautical Multi-carrier Communications", *2008 Integrated Comm. Navigation and Surveillance Conf. (ICNS 2008)*, Bethesda, MD, USA, May 2008

[4] C.-H. Rokitansky, M. Ehammer, Th. Gräupl, M. Schnell, S. Brandes, S. Gligorevic, C. Rihacek, and M. Sajatovic, "B-AMC - A system for future Broadband Aeronautical Multi-Carrier communications in the L-Band," *2007 Digital Avionics Systems Conference (DASC 2007)*, Dallas, TX, USA, October 2007, pp. 4.D.2-1- 4.D.2-13

[5] C.-H. Rokitansky, M. Ehammer, T. Gräupl, S. Brandes, S. Gligorevic, M. Schnell, C. Rihacek, and M. Sajatovic, "B-AMC – Aeronautical Broadband Communication in the L- band," in *Proc. CEAS European Air and Space Conference '07*, Berlin, Germany, Sept. 2007, pp. 487-496

[6] M. Sajatovic, B. Haindl, M. Ehammer, Th. Gräupl, M. Schnell, U. Epple, S. Brandes, "L-DACS1 System Definition Proposal", *Eurocontrol Study, Edition 1.0*, February 2009

[7] EUROCONTROL/FAA, "Communications Operating Concept and Requirements for the Future Radio System", *Ver. 2*, May 2007

[8] M. Schnell, S. Brandes, S. Gligorevic, M. Walter, C. Rihacek, M. Sajatovic, B. Haindl, "Interference Mitigation for Broadband L-DACS", *2008 Digital Avionics Systems Conference (DASC 2008)*, St. Paul, MN, USA, October 2008

[9] S. Brandes, U. Epple, S. Gligorevic, M. Schnell, B. Haindl, M. Sajatovic, "Physical Layer Specification of the L-band Digital Aeronautical Communications System (L-DACS1)", *Integrated*

Comm. Navigation and Surveillance Conf. (ICNS 209), Washington, D.C, USA, May 2009

[10] EUROCONTROL, "VDL Mode 2 Capacity Analysis through Simulations, WP3.B – NAVSIM Overview and Validation Results", *Edition 1.2*, October 2005

[11] D. Chu, "Polyphase Codes With Good Periodic Correlation Properties", *IEEE Transactions on Information Theory, pp. 531-532,* July 1972

[12] T. Schmidl, D. Cox, "Robust Frequency and Timing Synchronization for OFDM", *IEEE Transactions on Communication, Vol. 45, no. 12,* December 1997

[13] M. Sandell, J. van de Beek, P. Börjesson, "Timing and Frequency Synchronization in OFDM Systems Using the Cyclic Prefix", *Proc. of International Symposium on Synchronization, pp. 16-19*, Essen, Germany, December 1995

[14] S. Brandes, M. Schnell, "Interference Mitigation for the Future Aeronautical L-Band Communication System," in *7th International Workshop on Multi-Carrier Systems & Solutions (MC-SS 2009)*, Herrsching, Germany, May 2009, S. Plass et al., Ed., Springer, pp. 375-384.

Email Addresses

ulrich.epple@dlr.de

sinja.brandes@dlr.de

snjezana.gligorevic@dlr.de

michael.schnell@dlr.de